

# Duplexing Filtering Antenna for Wireless Communication Systems

Eugene Amobichukwu Ogbodo  
 <https://orcid.org/0000-0002-9798-723X>  
*University of Hertfordshire, UK*

Felix Ngobigha  
*University of Suffolk, UK*

Azunka Ukala  
*University of Hertfordshire, UK*

## ABSTRACT

The duplexer and antenna are vital components in the communication infrastructures such as satellites, base stations, synthetic aperture radars, etc. Traditionally, the duplexers and the antennas are separately designed before being cascaded into a system by impedance matching circuit. This technique leads to a larger size system and reduced performance as one or more of the components deteriorate. To avoid low performance in the system, an integrated duplexer and antenna can be used. This is a situation where the duplexer and the antenna are co-designed. The integration results in a less complex system as the feeding/matching circuits are no longer required and are replaced by a filter/duplexer. At this stage, the antenna acts as a resonator with radiating characteristics to the filter/duplexer resulting in response with low insertion loss and sharp skirts leading to good guard bands.

## KEYWORDS

Centre Frequency, Coupling, Filtering, Fractional Bandwidth, Matching Network, Polarisation, Quality Factors, Return Loss

## 1. INTRODUCTION

Parts of the main components in the wireless communication systems are filters, duplexers, and antennas. To design these components traditionally, different methods are applied to achieving them. This leads to having different specialists for these components. These includes filters (Ogbodo et al 2016, Ogbodo et al 2021, Tang et al 2023), duplexers (Ogbodo et al 2016, Nwajana and Yeo 2016, Wu et al 2016, Tang et al 2019, Anguera et al 2020, Ogbodo et al 2018, Ogbodo 2021) or antennas (Zhang et al 2022, Ogbodo et al 2021, Ahmed et al 2024, Imran et al 2024, Mohan et al 2024). In their respective design stages, for base station and or satellite communication systems, their input and output ports are assumed to be 50 Ohm interfaced. The reason is that if the interfaces are assumed to be 50 Ohms, the responses will be maintained after connection and commissioning. However, this is usually not the case during operation due to mismatches in the individual component specifications, leading to deteriorated performance. To avoid the deterioration in the systems performance, these components are co-designed, leading to more compact systems by avoiding the use of the mismatching circuits between the components. (Liu and Zhang 2024, Aly et al 2019, Wu et al 2019, Mao et al 2016, Mansour et al 2019, Liang et al 2023, Hasan and Shekhar 2024, Mahmud 2021).

DOI: 10.4018/IJECME.380489

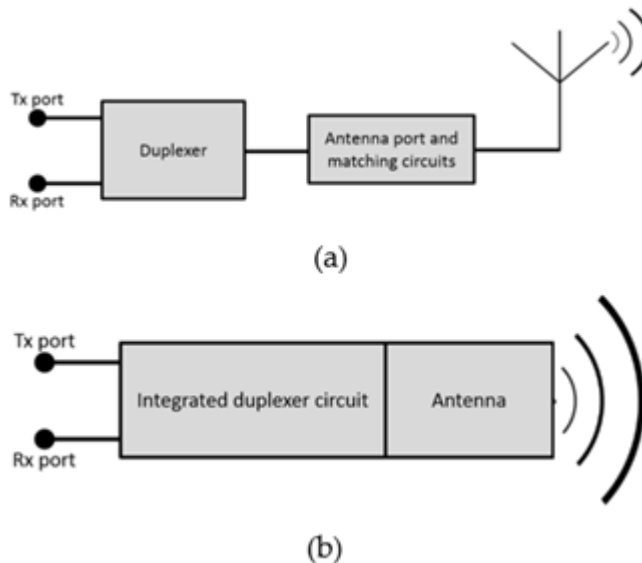
This article published as an Open Access article distributed under the terms of the Creative Commons Attribution License (<http://creativecommons.org/licenses/by/4.0/>) which permits unrestricted use, distribution, and production in any medium, provided the author of the original work and original publication source are properly credited.

In this work, co-designing of antenna and filter is presented leading to co-designing of duplexer and antenna. The method used reduced the complexity of the system by eliminating some of the feeding/matching circuits experienced in the conventional system (Mao et al 2015, Eltokhy and Wang 2016). It involves replacing the feeding network of the antenna with filters. This led to all resonant structures in the system and elimination of the insertion losses normally introduced by the interconnections between antennas and filters. In addition to this, the easy control of the bandwidths is achieved by varying the coupling gap between the resonant poles of the resonators (Liu and Zhang 2024, Mao et al 2015). That is resonators of the filters and the resonating element of the antenna.

In the wireless communication systems, duplexers are used as a link between the transmitter (Tx), and receiver (Rx), and provides the opportunity for both components to share one antenna port. To avoid interference, high isolation is required between the Tx channel port and the Rx channel port of the duplexer component. Figure 1(a) displays the duplexer and antenna connection in a conventional topology. Figure 1(b) displays the topology of co-designing of a duplexer and antenna as proposed. This method avoids the need to have the 50 Ohm interface matching network and the cable joining the duplexer and the antenna. This is the integrated system.

The first proposed work is the co-designing of a bandpass filter and an orthogonal mode of a patch antenna. For ease of implementation, the general filter synthesis is employed. The orthogonal modes of the antenna are 1.8 GHz and 2.4 GHz. These modes were focused on during the designs which yielded a 1.8GHz filtering antenna and a 2.4 GHz filtering antenna.

Figure 1. Duplexer and antenna: (a) conventional topology subsystem, (b) co-designed system



The co-designing of the antenna and duplexer is to demonstrate the multi-functional of RF front end of the wireless communications component. To demonstrate this, the orthogonal mode of the patch antenna is used to function as a resonating junction, radiating junction, signal splitter and combiner in the duplexer-antenna component. Two sets of three-poles bandpass filter were individually designed to operate at the orthogonal modes of the patch antenna, which are 1.8 GHz and 2.4 GHz. After each of the bandpass filter were fully designed and optimized, their third resonators were removed and replaced with the patch antenna. It is worth mentioning that the patch antenna were treated as a resonator during the coupling with the individual filters. However, the quality external

factors ( $Q_{ext}$ ) of the third resonators were at this time performed on the patch antenna as quality radiation factor ( $Q_{rad}$ ). This method led to compactness or miniaturized circuit because the 50 Ohm interface and matching network is not needed. In addition to this, the patch antenna acted as a radiating element while its orthogonal modes reduced the number of required resonators from six to five and the antenna forming an integral part of the component. This method is different from (Mao et al 2019), where coupling is achieved using the through hole coupling method leading to stack formation. In this design, the coupling is achieved using the edge coupling method and co-designed on a single substrate which formed the main contribution of this work. In (Hasan 2024), a compact full-duplex antenna was presented. It consists of two identical patches which acted as antennas, although the design presented some level of reasonable isolation, the circuit was big. In addition to the size, the design lacks filtering capability which will even make it bigger if implemented. Even though the patches were placed in close proximity and connected through a neutralization line in a bid to enhance isolation between the patches, the achieved isolation was less than -8dB between the antennas.

## 2. DUPLEXING ANTENNA DESIGN

### 2.1. Design Specifications

To proceed with this proposal, the lumped element filtering synthesis was first utilized. The numerical calculation used is focused on the duplexer specifications of Rx and Tx at 1.8 GHz and 2.4 GHz for GSM and WIFI channels respectively. They both operate at 4% FBW that is Rx from 1.764 GHz to 1.836 GHz, and Tx channel from 2.352 GHz to 2.448 GHz. Return loss is set at -20 dB for both channels and with three-poles on Chebyshev ripple factor of 0.043 dB with low-pass prototype response obtained from (Ogbodo et al 2017, Ogbodo et al 2018, Werfelli 2016). The terminal immittances of the low-pass prototype responses were provided as the  $g$ -values, with  $g_0 = g_4 = 1.0$ ,  $g_1 = g_3 = 0.8516$  and  $g_2 = 1.1032$ . This  $g$ -values were numerically used to achieve the capacitive and inductive values of the lumped element components, and the  $J$ -inverter values used for frequency transformation purposes.

The Equations (1a) and (1b) were used to obtain the capacitive and inductive values of the resonant frequency of the lumped element components, respectively. Whereas the equations (2a), (2b), and (2c) are used for evaluating the  $J'$ -inverter values of  $J'_{01}$ ,  $J'_{12}$ , and  $J'_{23}$  of the lumped elements respectively. To obtain the capacitive coupling values, the  $J'$ -inverter values had to go through a frequency transformation by dividing them with  $w_0$  (3), this frequency transformation yielded the capacitive coupling values as shown in Table-1. The Table-1 shows the obtained values from equations (1) and (2). These values were used for the lumped element model of the design shown in Fig. 2(a) and in Fig. 3(a) for the channel filtering antennas and the Duplexer antenna respectively. The Figs. 2(b) and 2(c) shows the simulated responses of Fig. 2(a) for Rx and Tx channels filtering antenna respectively. While the Fig. 3(b) shows the simulated response of the Fig. 3(a).

Table 1. Calculated parameters from equations (1), and (2)

Channel	C pF	L nF	J01 pF	J23 pF	FBW %	wo
2.4 GHz	28.2334	0.155759	1.32629	1.16526	0.04	1.131E10
1.8 GHz	37.6446	0.207679	1.76839	1.55368	0.04	1.508E10

Figure 2. (a) Filtering antenna channel; (b) Rx channel response; (c) Tx channel response

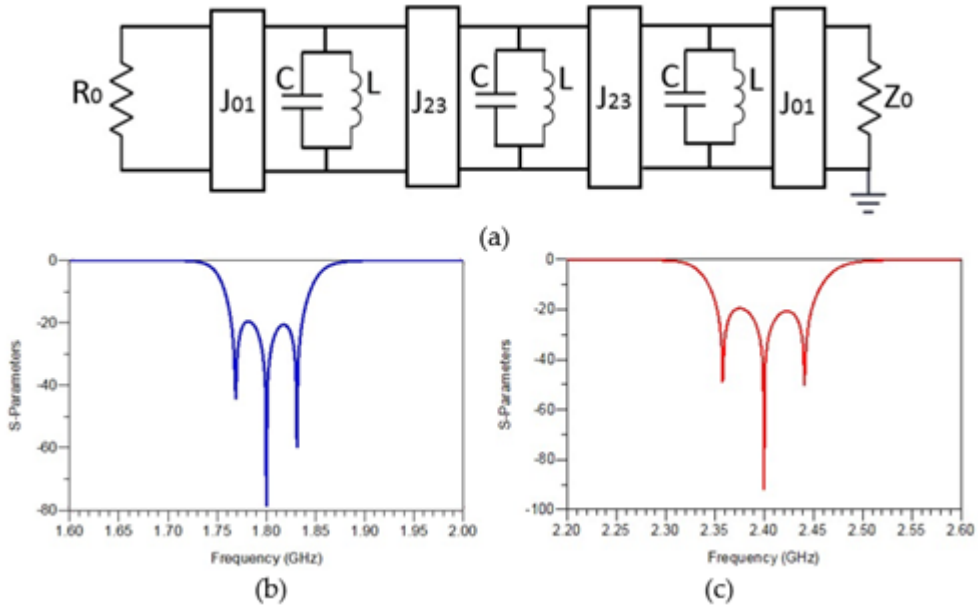
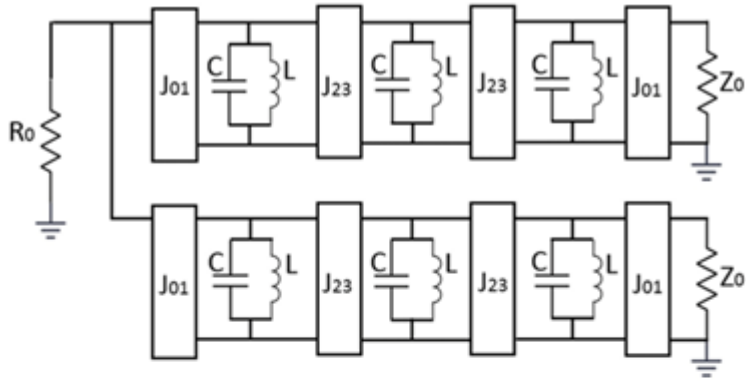
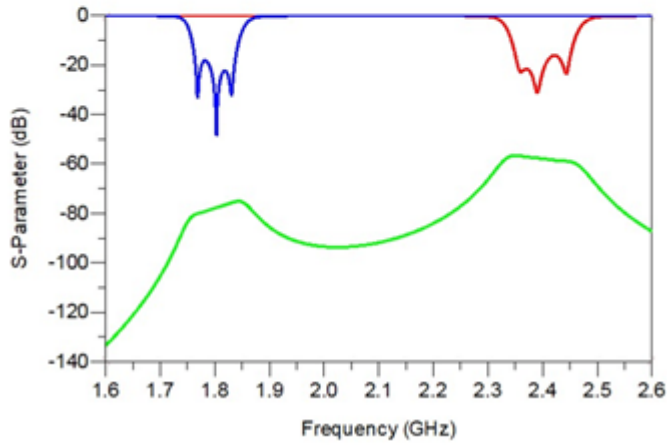


Figure 3. Duplexer antenna (a) schematic diagram; (b) duplexing antenna response



(a)



(b)

From the response, three poles could be seen in the return losses which confirms the contribution of the orthogonal modes of the patch antenna as resonance modes in the design and its inclusion that led to the reduction of the resonators from six to five in the filter designs. However, considering the fact that the antenna is an integral part of the design, the number is reduced from seven to five when compared with its equivalent conventional counterpart.

$$C = \frac{g_1}{w_0 Z_0 FBW} \quad (1.1)$$

where  $w_0 = 2\pi f_0$  and  $f_0$  is the fundamental frequency,

$$L = \frac{Z_0 FBW}{w_0 Z_0 FBW} \quad (1.2)$$

$$J_{01} = \frac{g_0}{Z_0} \quad (2.1)$$

$$J_{12} = \frac{J_{23}}{\sqrt{2}} \quad (2.2)$$

$$J_{23} = \frac{\sqrt{\frac{g_1^2}{g_1 g_2}}}{Z_0} \quad (2.3)$$

The next step is the transformation of the lumped element circuit to a distributed element circuit. This is to further confirm the proposed design. As the proposed design makes use of two channel filters linked together with a resonating antenna, the filters have the criteria mentioned above, with lowpass prototype obtained from (Liu and Zhang 2024, Aly et al 2019, Wu et al 2019). The g-values were used to obtain the coupling coefficient, (M) and the input/output quality factors (Q<sub>ex</sub>) used for the design of the filters using (3) and (4) respectively (Wu et al 2019, Mao et al 2013, Mansour et al 2019). The width (W) and the length (L) of the patch antenna are achieved from (5) (Liang et al 2023). The antenna, being a rectangular patch, possesses a dual-mode response at 1.8 GHz and 2.4 GHz depending on the feeding position used. If it is fed from the side of the width, it produces 1.8 GHz and when fed of the side of the length, it produces 2.4 GHz.

$$M_{n, n+1} = \frac{FBW}{\sqrt{g_1 g_2}} \quad (3)$$

$$Q_{ex} = \frac{g_0 g_1}{FBW} = 21.29 \quad (4)$$

$$W = \frac{C_0}{2f_0 \sqrt{\frac{\epsilon_r + 1}{2}}} \quad (5.1)$$

$$L_{eff} = \frac{C_0}{2f_0 \sqrt{\epsilon_{eff}}} - 2 \Delta l \quad (5.2)$$

where  $\epsilon_r$  is the dielectric constant,  $C_0$  is the speed of light in free space and  $L_{eff}$  is the effective length of the resonant element,  $\epsilon_{eff}$  is the effective dielectric constant, and  $\Delta l$  is the line extension and expressed as:

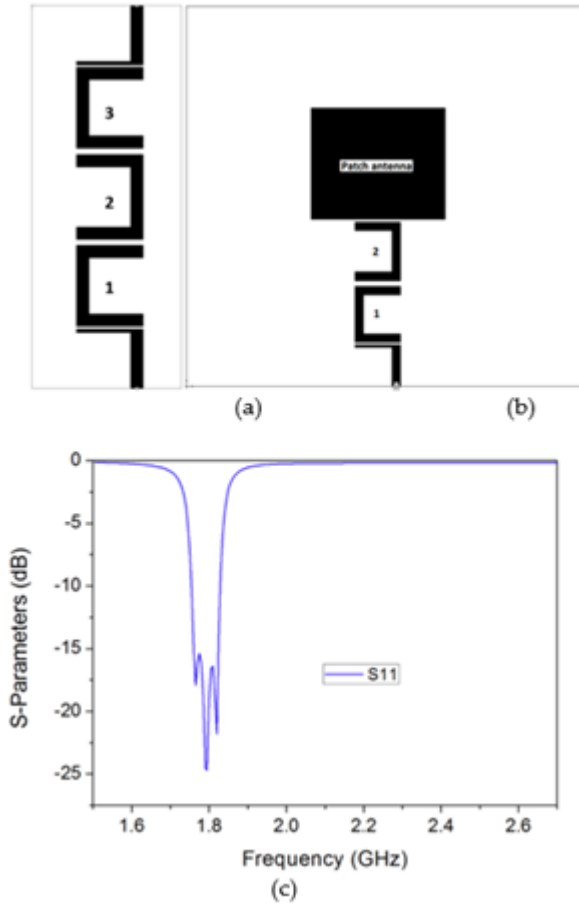
$$\Delta l = 0.412h \left[ \frac{0.262 + \frac{w}{h}}{0.813 + \frac{w}{h}} \right] \left[ \frac{\epsilon_{eff} + 0.3}{\epsilon_{eff} - 0.258} \right] \quad (5.3)$$

To preserve the filtering characteristics of the filters, the Q<sub>rad</sub> of the patch antenna is made to have the same value as the Q<sub>ext</sub> of the filters input. Because of this, the patch's radiated power or gain response follows similar pattern of the insertion loss response of the filter with minimum insertion loss in the passband but with high rejection in the off band or low gain.

## 2.2. Filtering Antenna Configuration

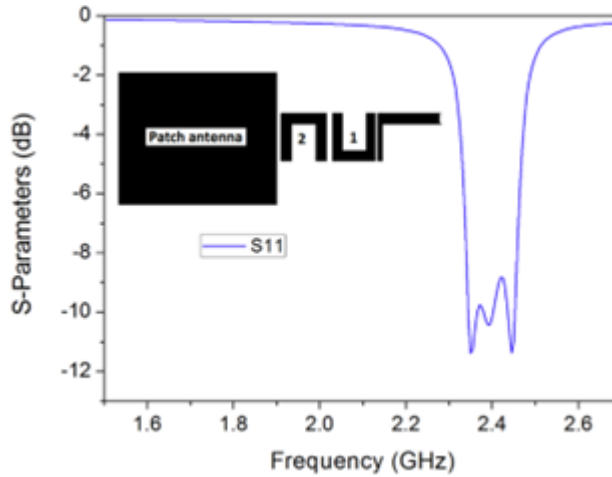
To demonstrate the filtering antenna configuration in the co-design process. Each channel of the duplexing antenna is designed separately by co-designing the patch antenna with its corresponding channel filter in the orthogonal modes individually. Firstly, the Rx of 1.8 GHz three-poles hairpin filter had its third resonator replaced with the patch antenna as provided in Figure 3. The coupling coefficient of the resonator 2 and the patch antenna is made to be the same as that of the coupling coefficient of the resonator 2 and resonator 3 of the filter shown in Figure. 4(a). After extracting the coupling distance, the filter and the antenna components are then assembled and optimised to specification as provided in Figure 4(b). Figure 4(c) shows the simulated response of the filtering antenna configuration after optimisation.

Figure 4. 1.8 GHz channel (a) filter layout; (b) filtering antenna layout; (c) filtering antenna response



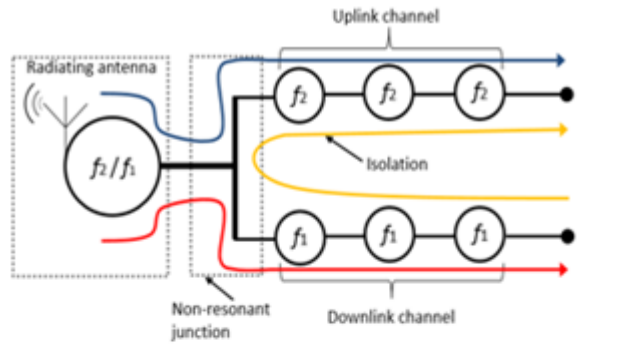
This same process used in designing the 1.8 GHz filtering antenna is used to design the filtering antenna of the second mode operating at 2.4 GHz. This process also maintained the in-line coupling of the patch antenna with the 2.4 GHz filter in the corresponding orthogonal mode. It also replaced the third resonator of the filter with the patch antenna and then optimised. Figure 5 presents the topology of the 2.4 GHz filtering antenna after optimization as an insert in its achieved simulated response. After both filtering antennas are achieved. The orthogonal modes of the patch antenna are used to combine the two filtering-antennas into a duplexing antenna.

Figure 5. The 2.4 GHz filtering antenna layout as an insert in its simulated return loss (S11) response

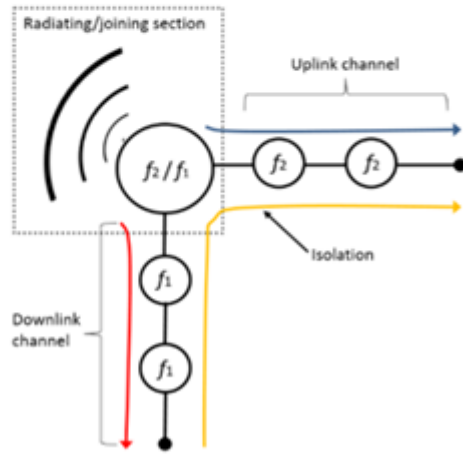


The 1.8 GHz channel serves the receiving (Rx) for the downlink whilst the 2.4 GHz channel serves the transmitting (Tx) channel for the uplink. Figure 6(a) presents the coupling configuration of the duplexing antenna in a conventional cascaded design whilst Figure 6(b) presents the proposed coupling topology. The EM software Sonnet is used for the simulation and the proposed design layout is presented in Figure 7 with the achieved dimensional parameters after optimisation. The design prototype is fabricated on Rogers RO4003C substrate with a dielectric constant of 3.55, thickness of 1.524 mm, and loss tangent of 0.0029 (nominal value at 10 GHz) and presented as an insert in the Figure 7 indicating the achieved physical dimension after optimisation. The LPKF ProtoMat S63 micro-milling process was used for the fabrication.

Figure 6. Coupling topology of duplexing antenna (a) conventional; (b) proposed

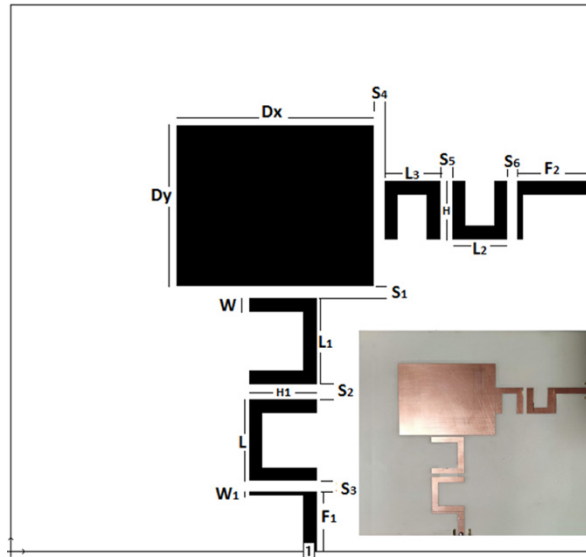


(a)



(b)

Figure 7. Designed duplexing antenna layout with parameters.  $D_x = 52.5$  mm,  $D_y = 43$  mm,  $S_1 = 1.05$  mm,  $S_2 = 2.1$  mm,  $S_3 = 0.3$  mm,  $S_4 = 0.25$ ,  $S_5 = 2$  mm,  $S_6 = 0.3$  mm,  $F_1 = 15$  mm,  $F_2 = 20$  mm,  $H = 15.5$  mm,  $H_1 = 17.9$  mm

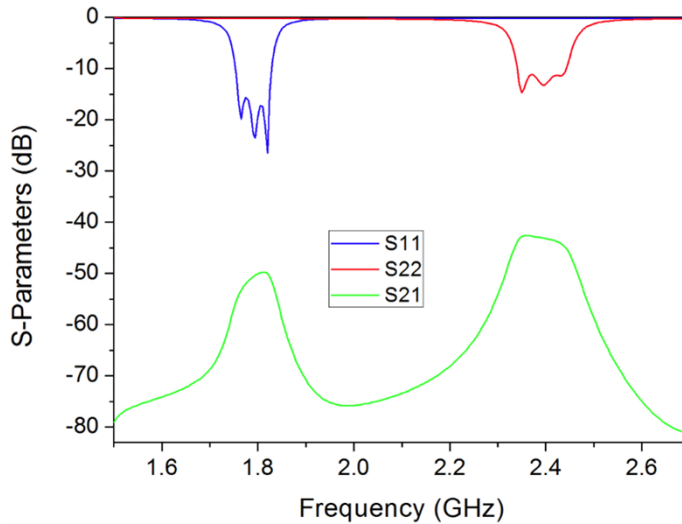


### 3. EXPERIMENTAL RESULTS

#### 3.1. Simulated and Measured Results

The simulated S-parameters of the optimised duplexing antenna is presented in Figure 8 where it presents the Rx channel measured and started from 1.764 GHz to 1.836 GHz while the Tx channel is measured and started from 2.352 GHz to 2.448 GHz. This shows that this design achieved the proposed 4% FBW on the individual channels. The sharp skirts normally observed in co-designed filtering antenna response is well noticed in both channels. The return losses are at -17 dB and -13 dB respectively. Also, the isolation between the two channels (ports S21) is at about -51dB on the Rx channel and at -43 dB at the Tx channel. As shown in Figure 8, the isolation S21 in comparison with S11 and S22 depicts a good isolation between the channels. It can also be observed that the three poles for each channel are clearly identifiable in the Figure 8 which indicates the contribution of the antenna as a resonant pole for each channel (Rx and Tx). In comparison with the lumped element circuit shown in Figure 3(b), it is observed that the lumped element circuit and the distributed element circuit agree with each other. It also confirms the correctness of the lumped element configuration shown in Figure 3(a).

Figure 8. Measured duplexer antenna isolation between two channels (ports) and the frequency responses



Figures 9 and 10 represent the measured far-field radiation patterns for co- and cross-polarisations at 1.8 GHz and 2.4 GHz, respectively. Clearly, the maximum far-field signal strength or maximum directivity achieved with the proposed duplexing antenna approach for the E-plane at 1.8 GHz (cross-polarisation) and the E-plane at 2.4 GHz (co-polarisation) suggests a significant margin of about -53 dB at zero degrees. This shows the contribution of the antenna as a resonant pole for each channel (Tx and Rx). Furthermore, the polarisation isolation between the cross-polarisation and co-polarisation is about 22 dB at an azimuth angle of zero degree as shown in Figure 8. Whilst the measured far-field radiation patterns at the H-plane for both co-polarisation at 1.8 GHz and cross-polarisation at 2.4 GHz results in undesirable radiation patterns with noticeable polarisation isolation around 320 degrees as highlighted in Figure 9 with the likelihood of reduced performance. It is assumed that the discrepancies noticed in the far-field radiation patterns of Figure 9 and 10 as well as S-parameters of Figure 8 are associated with fabrication tolerance, post fabrication tuning, and the variation of the dielectric constant for the high permittivity dielectric material of Rogers RO3004C. The used material has a dielectric constant of 3.38, dissipation factor of 0.0023, copper clad, and high thermal stability of  $T_g > 280^\circ\text{C}$ .

Figure 9. Measured far-field radiation patterns on the E-plane at 1.8 GHz (cross-pol) and 2.4 GHz (co-pol)

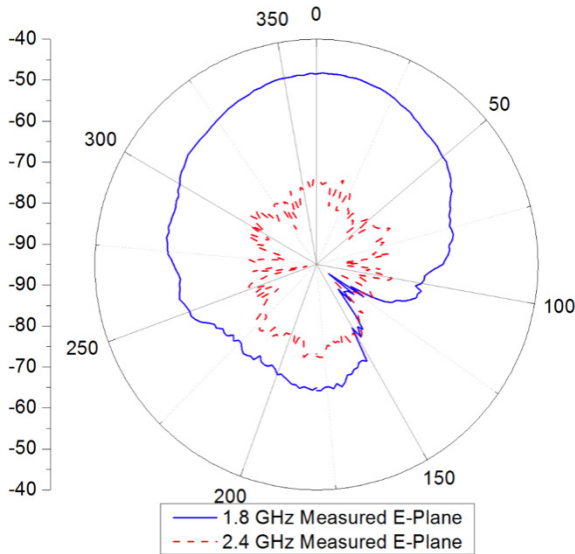
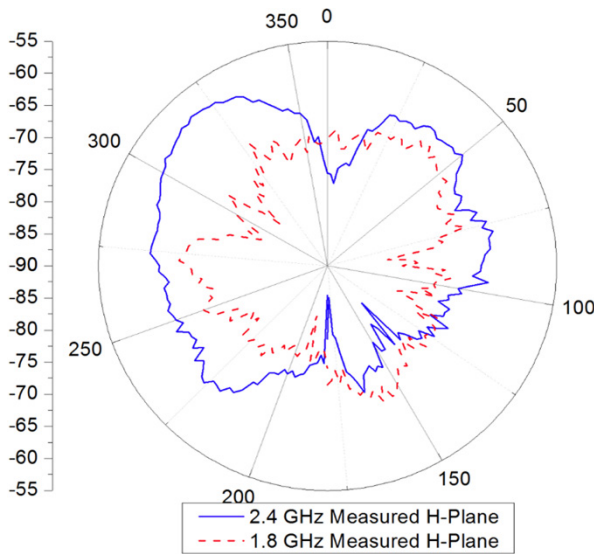


Figure 10. Measured far-field radiation patterns on the H-plane at 1.8 GHz (Co-pol) and 2.4 GHz (cross-pol)



#### 4. CONCLUSION

In this study, we demonstrated how the proposed duplexing antenna design proved to provide good filtering characteristics. The achieved sharp skirts seen at the band edges indicate that this design has good guard bands. This enhanced feature is because of the integration of the duplexer and the antenna which led to the elimination of the impedance matching circuits between them such as the 50 Ohm interface matching network. The method used in this design made use of all the resonators including the antenna to contribute to the filtering functions because the antenna is treated as a resonator. The integration process utilised the general filter synthesis procedure making it easy to implement. This

strategy helped to address the difficulties in achieving the desired bandwidth, radiation efficiency and the fabrication tolerance when designing integrated circuits. This is mainly due to the use of general filter syntheses and the coupling method used. The two bands of the duplexing antenna operate on orthogonal polarisations. This makes this design to be suitable for applications where polarisation diversity is required.

## **CONFLICTS OF INTEREST**

We wish to confirm that there are no known conflicts of interest associated with this publication and there has been no significant financial support for this work that could have influenced its outcome.

## **FUNDING STATEMENT**

No funding was received for this work.

## **PROCESS DATES**

Received: December 8, 2024, Revision: April 10, 2025, Accepted: April 11, 2025

## **CORRESPONDING AUTHOR**

Correspondence should be addressed to Eugene Ogbodo; eugene.ogbodo@gmail.com

## REFERENCES

- Ahmad, S., Ogbodo, E., & Ukala, A. (2024, Apr). Enhanced Dual-band Antenna for Intelligent Vehicular Communications. In *2024 Photonics & Electromagnetics Research Symposium (PIERS)* (pp. 1-7). IEEE. DOI: 10.1109/PIERS62282.2024.10618202
- Ali, A. E. T., & Wang, Y. (2016, Nov). Integrated filtering planar dipole antenna using edge coupled feed. In *2016 Loughborough Antennas & Propagation Conference (LAPC)* (pp. 1-4). IEEE. DOI: 10.1109/LAPC.2016.7807494
- Aly, M. G., Mao, C., Gao, S., & Wang, Y. (2019). A Ku-band filtering duplex antenna for satellite communications. *Progress in Electromagnetics Research M. Pier M*, 85, 1–10. DOI: 10.2528/PIERM19071506
- Anguera, J., Andújar, A., & Jayasinghe, J. (2020). High-Directivity Microstrip Patch Antennas Based on TModd-0 Modes. *IEEE Antennas and Wireless Propagation Letters; Volume: 19, Issue: 1*.
- Hasan, M. N., & Shekhar, S. (2024, Jul). A Compact Full-duplex Antenna with High Isolation Using Neutralization Line. In *2024 IEEE International Symposium on Antennas and Propagation and INC/USNC-URSI Radio Science Meeting (AP-S/INC-USNC-URSI)* (pp. 1959-1960). IEEE. DOI: 10.1109/AP-S/INC-USNC-URSI52054.2024.10687018
- Hong, J. S. G., & Lancaster, M. J. (2004). *Microstrip filters for RF/microwave applications*. John Wiley & Sons.
- Imran, A. Z. M., Thomas, M., Ogbodo, E., & Ukala, A. (2024, Apr). ITS-G5 Antennas: Powering Future Urban Transports. In *2024 Photonics & Electromagnetics Research Symposium (PIERS)* (pp. 1-6). IEEE.
- Liang, Y. Z., Chen, F. C., Xiang, K. R., & Zeng, W. F. (2023). Wideband co-polarized stacked patch antenna for in-band full-duplex applications. *IEEE Transactions on Antennas and Propagation*, 71(12), 9920–9925. DOI: 10.1109/TAP.2023.3319371
- Liu, J., & Zhang, P. (2024). An ultra-small wideband diplexer with triangular-shaped and rectangular-shaped resonators for mobile base stations. *Electrical Engineering*, 1–18.
- Mahmud, R. H., & Lancaster, M. J. (2021). A 2 × 2 Filtering subarray element antennas using all-resonator structures. *IET Microwaves, Antennas & Propagation*, 15(6), 592–599. DOI: 10.1049/mia2.12080
- Mansour, G., Nugoolcharoenlap, E., Lancaster, M. J., & Akkaraekthalin, P. (2019, Dec). Comparison of different order filtering antennas. In *2019 Research, Invention, and Innovation Congress (RI2C)* (pp. 1-5). IEEE. DOI: 10.1109/RI2C48728.2019.8999887
- Mao, C. X., Gao, S., Wang, Y., Qin, F., & Chu, Q. X. (2016). Compact highly integrated planar duplex antenna for wireless communications. *IEEE Transactions on Microwave Theory and Techniques*, 64(7), 2006–2013. DOI: 10.1109/TMTT.2016.2574338
- Mao, C. X., Gao, S., Wang, Z. P., Wang, Y., Qin, F., Sanz-Izquierdo, B., & Chu, Q. X. (2015, Apr). Integrated filtering-antenna with controllable frequency bandwidth. In *2015 9th European Conference on Antennas and Propagation (EuCAP)* (pp. 1-4). IEEE.
- Mohan, M., Ukala, A., Ogbodo, E., & Imran, A. Z. M. (2024, Feb). A Novel Single-Band Antenna for Enhanced V2X Communication: Review Towards Prototype Development. In *International Congress on Information and Communication Technology* (pp. 371-380). Singapore: Springer Nature Singapore. DOI: 10.1007/978-981-97-3556-3\_30
- Nwajana, A. O., & Yeo, K. S. (2016, Oct). Multi-coupled resonator microwave diplexer with high isolation. In *2016 46th European Microwave Conference (EuMC)* (pp. 1167-1170). IEEE. DOI: 10.1109/EuMC.2016.7824556
- Ogbodo, E., Wang, Y., & Yeo, K. S. (2016). Microstrip dual-band bandpass filter using U-shaped resonators. *Progress in Electromagnetics Research Letters*, 59, 1–6. DOI: 10.2528/PIERL15072303
- Ogbodo, E. A. (2021). Comparative Study of Transmission Line Junction vs. Asynchronously Coupled Junction Dplxers. In *Handbook of Research on 5G Networks and Advancements in Computing, Electronics, and Electrical Engineering* (pp. 326-336). IGI Global. DOI: 10.4018/978-1-7998-6992-4.ch013
- Ogbodo, E. A., Aly, M. G., Ali, A. E. T., Wu, Y., & Wang, Y. (2018). Dual-band filtering antenna using dual-mode patch resonators. *Microwave and Optical Technology Letters*, 60(10), 2564–2569. DOI: 10.1002/mop.31396

Ogbodo, E. A., Ngobigha, F., Obadijah Ali, N., & Atuba, S. (2021). A diplexer with direct coupled resonant junction. *Microwave and Optical Technology Letters*, 63(6), 1677–1681. DOI: 10.1002/mop.32787

Ogbodo, E. A., & Nwajana, A. O. (2021, Jun). A bandpass filter using edge coupled and direct coupled techniques. In *2021 International Conference on Electrical, Communication, and Computer Engineering (ICECCE)* (pp. 1-4). IEEE. DOI: 10.1109/ICECCE52056.2021.9514068

Ogbodo, E. A., Wu, Y., Callaghan, P., & Wang, Y. (2017). A compact diplexer with a split-ring resonator junction. *Microwave and Optical Technology Letters*, 59(9), 2385–2390. DOI: 10.1002/mop.30740

Ogbodo, E. A., Wu, Y., Callaghan, P., & Wang, Y. (2017). Asynchronously coupled resonant junctions for diplexers and multiport filtering networks. *Microwave and Optical Technology Letters*, 59(12), 3046–3051. DOI: 10.1002/mop.30877

Ogbodo, E. A., Wu, Y., Callaghan, P., & Wang, Y. (2018, Sep). Masthead combiner employing asynchronously coupled resonant junctions. In *2018 48th European Microwave Conference (EuMC)* (pp. 695-698). IEEE. DOI: 10.23919/EuMC.2018.8541754

Ogbodo, E. A., Wu, Y., & Wang, Y. (2016, Oct). Microstrip diplexers with dual-mode patch resonant junctions. In *2016 46th European Microwave Conference (EuMC)* (pp. 1155-1158). IEEE. DOI: 10.1109/EuMC.2016.7824553

Ogbodo, E. A., Wu, Y., & Wang, Y. (2017, May). Dual-path dual-band filters based on patch resonators. In *2017 International Workshop on Electromagnetics: Applications and Student Innovation Competition* (pp. 67-68). IEEE. DOI: 10.1109/iWEM.2017.7968779

Tang, C. W., & Jiang, J. M. (2023, Jun). Design of a microstrip dual-/quad-band switchable bandpass filter with dual-band bandpass filters. In *2023 IEEE/MTT-S International Microwave Symposium-IMS 2023* (pp. 948-950). IEEE. DOI: 10.1109/IMS37964.2023.10188217

Tang, Z., Liu, J., Lian, R., Li, Y., & Yin, Y. (2018). Wideband differentially fed dual-polarized planar antenna and its array with high common-mode suppression. *IEEE Transactions on Antennas and Propagation*, 67(1), 131–139. DOI: 10.1109/TAP.2018.2878284

Werfelli, H., Tayari, K., Chaoui, M., Lahiani, M., & Ghariani, H. (2016, Mar). Design of rectangular microstrip patch antenna. In *2016 2nd International Conference on Advanced Technologies for Signal and Image Processing (ATSIP)* (pp. 798-803). IEEE. DOI: 10.1109/ATSIP.2016.7523197

Wu, Y., Wang, Y., & Ogbodo, E. A. (2016, Oct). Microstrip wideband diplexer with narrow guard band based on all-resonator structures. In *2016 46th European Microwave Conference (EuMC)* (pp. 1163-1166). IEEE. DOI: 10.1109/EuMC.2016.7824555

Wu, Z., Chen, J., Zhang, A., Lu, X., & Zhang, X. (2019). Design of dual-mode dual-band rectangular waveguide filtering antenna. *International Journal of RF and Microwave Computer-Aided Engineering*, 29(7), e21727. DOI: 10.1002/mmce.21727

Zhang, Y., Lin, X. J., & Gu, W. D. (2022). A three-state diplexer design using stub-loaded resonator pairs. *Microwave and Optical Technology Letters*, 64(11), 1923–1930. DOI: 10.1002/mop.33400

*Eugene Ogbodo has made significant contributions to the field of microwave engineering through research and innovation in several areas: Miniaturization of Microwave Devices: He has worked extensively on reducing the size of microwave components for use in modern communication systems, improving the compactness and efficiency of these devices. Satellite Communication Systems: His research has advanced technologies for satellite communication, particularly focusing on improving signal clarity and transmission efficiency. Integration of Passive Microwave Devices: His work in integrating passive components has enhanced the performance of base stations and other communication infrastructures. Dr. Ogbodo's published work has influenced the design and development of microwave circuits, contributing to both academic advancements and industrial applications. His research has been pivotal in increasing the functionality of high-frequency devices used in satellite and wireless communication systems.*